*J. Fluid Mech.* (1981), *vol.* 105, *pp.* 261–281
*Printed in Great Britain*



# Properties of the large structure in a slightly heated turbulent mixing layer of a plane jet

By S. RAJAGOPALAN AND R. A. ANTONIA
Department of Mechanical Engineering, University of Newcastle, N.S.W., 2308, Australia

(Received 5 November 1979 and in revised form 21 July 1980)

The convection speed and average inclination of the large structure in the turbulent mixing layer of a plane jet have been obtained using different techniques. Ensemble-averaged shapes of the signatures of velocity and temperature associated with this structure are also presented. An array of cold wires is used to simultaneously observe the temperature fluctuation $\theta$ at several points in space. A cold-wire/X-wire combination is used to measure $\theta$, the streamwise $u$ and the normal $v$ velocity fluctuations. The front of the structure moves faster than the back and the average inclination of this structure to the jet axis is approximately 40°. A detection scheme, based on positive peaks of the cubed values of the temperature derivative, is used to identify the large structure and obtain average signatures of $\theta$, $u$, $v$, and of the products $uv$, $u\theta$ and $v\theta$. These signatures are consistent with a vortex-like description of the large structure. They also reflect the existence of a thin interconnecting region or 'braid' between two consecutive vortical structures. This region is identified by the sharp changes in temperature and is interpreted as part of the large structure. In the central part of the mixing layer, at least 80 % of the Reynolds shear stress and 50 % of the average normal heat flux appear to be contributed by the large structure.

## 1. Introduction

The idea that large-scale coherent structures containing concentrated regions of vorticity play an important role in turbulent shear flows has been frequently mentioned and discussed over the last few years. A summarized account of contributions to the study of coherent structures in turbulence was given by Davies & Yule (1975). They concluded that the available experimental evidence made it quite clear that these structures play a dominant role in the shear flow development and that greater insight can be obtained into turbulent mixing by studying the development of these structures and their interaction.

Particular attention has been given to the properties of coherent, large structures in the mixing region of circular and two-dimensional jets in view of the relative importance of these structures to turbulent transport phenomena, entrainment and jet noise. The presence of vortex-like large structures in circular and two-dimensional mixing layers seems now well established and features such as the amalgamation or pairing and indeed the disintegration or disappearance of these structures, are being studied by different investigators. From flow visualization studies of the large structure in an axisymmetric mixing layer, Hussain & Clark (1981) concluded that organized large structures were formed only occasionally and that tearing was as prevalent as pairing.

A brief summary of the main results of relevant mixing-layer investigations is given below.

In a two-stream mixing layer, Brown & Roshko (1974) observed well-defined vortex-like coherent structures at a moderate Reynolds number. From flow visualization studies, they suggested that entrainment and mixing occur on a scale of the size of the large structure. Dimotakis & Brown (1976) observed rapid mixing during the amalgamation of large structures in a turbulent mixing layer in a water channel. The fundamental periodicity, estimated from autocorrelations of the velocity fluctuation, was observed to scale with the distance from the virtual origin and the convection velocity of the large structure.

The average signature of the large structure has been determined, using conditional sampling techniques, by Browand & Weidman (1976), Winant & Browand (1974), Bruun (1977), Yule (1978) and Lau & Fisher (1975). Most of the techniques used to detect the large structure are based on the spike-like nature of the velocity signals at the edges of the mixing layer. Using a hot-film probe as the detector measuring $u$ and a second probe for sampling, Winant & Browand (1974) obtained ensemble-averaged shapes of $u$ at different points in a mixing layer formed downstream from a splitter plate in a water channel. Sampling was triggered when the velocity sensed by the detection wire exceeded a threshold level with either a positive or negative slope. Ensemble averages of $u$ indicated the existence of a coherent structure with a phase difference on either side of the layer. Pairing of the large-scale structure was observed to control the growth of the mixing layer. Using combined flow visualization and hot-film measurements, Browand & Weidman (1976) (see also Browand 1975) obtained ensemble-averaged signatures of $u$, $v$, $uv$ and ensemble-averaged isovorticity contours during and after pairing. In either situation, the maximum ensemble-averaged vorticity was about 90 % greater than the maximum conventional time-mean vorticity. Significant quantitative production of Reynolds stress was observed to be associated with the pairing interactions.

Using the sharp, spike-like appearance of the velocity $u$ near the core and near the low-speed side of the mixing layer of a circular jet to identify the passage of the large structure, Lau & Fisher (1975), Bruun (1977) and Yule (1978) made conditionally sampled velocity measurements. In Lau & Fisher's experiments, two hot-wire probes were used for triggering and sampling. The triggering probe was kept near the potential core or near the low-speed side while the sampling wire, which was downstream of the triggering probe, was moved across the mixing layer. At a station $x/d = 2$ ($d$ is the nozzle diameter) downstream of the nozzle exit, $u$ exhibited a negative spike at $r/d = 0{\cdot}4$ (radial distance $r$ is measured from the jet axis) and a positive spike at $r/d = 0{\cdot}6$. Lau & Fisher concluded that this technique revealed the vortex-like character of the large structure. Bruun (1977) used positive and negative peaks of $u$ to trigger the sampling probe in order to establish the relationship between the large positive peaks and a rapidly moving large structure and between the large negative peaks and a slowly moving large structure. Using flow visualization and conditional sampling, Yule (1978) concluded that vortex rings in a round jet are present over a short, transitional region near the nozzle but not in the fully developed mixing-layer region.

Sokolov, Hussain & Kleis (1979) studied the structure of an artificially introduced turbulent spot in the mixing layer of a circular jet with the aim of understanding the

evolution of a naturally occurring coherent, large structure. Hussain & Zaman (1980) have investigated the large-scale structure in the near field of a circular jet using pure-tone acoustic excitation. Two interesting results obtained (with a laminar exit boundary layer) are that the Reynolds stress due to the coherent structure is much larger than that due to background turbulence in the region $0 < x/d \lesssim 3$, and the zone average of the coherent-structure Reynolds stress over the cross-section of the merging vortex pair is larger than that over a single vortical structure either before or after the completion of pairing. While the eduction of the large structure is considerably simplified either by the introduction into the flow of a regular disturbance such as a spot or by acoustic excitation, caution must be used in interpreting features of the naturally occurring large structure in an unseeded or non-stimulated turbulent flow. The benefits to turbulence research of an approach based on the controlled excitation of the flow would depend on the ability of the users of this approach to show that the excitation does not create an artificial structure but simply triggers a naturally occurring one.

There appear to have been only a few investigations, e.g. Fiedler (1974, 1975) and Sunyach (1971), of the large structure in a slightly heated mixing layer. This is a little surprising since the idea of tagging parts of the fluid with a passive scalar, like heat, has been used effectively in other flows (e.g. in the turbulent boundary layer by Chen & Blackwelder 1978, and Subramanian & Antonia 1979) to study properties of the large structure. In particular, this idea should shed some light on the paths of fluid particles that are mixed by the presumably vigorous turbulent diffusion within the large structure. Sunyach (1971) used a rake of six temperature wires to observe the instantaneous temperature variation with time across the mixing layer of two streams with a temperature difference of 25 °C. With the rake in the central part of the layer, sharp temperature gradients were almost simultaneously recorded on all wires. Fiedler (1975) studied the turbulence structure of a mixing layer (maximum temperature difference across the layer was 26 °C) with an array of ten cold wires. Simultaneous traces of the temperature fluctuation, $\theta$, revealed, as in Sunyach's case, the occurrence of sharp temperature gradients that are at times traceable right across the layer and seem to demarcate convincingly the transition between vortical and non-vortical fluid. It should be noted that these large temperature jumps, which are associated with sharp shear zones at the outer boundaries of large structures rotating with the mean vorticity of the shear flow, have been observed in other flows (e.g., boundary layer, jets; see Gibson, Friehe & McConnell 1977). In fact, there seems little doubt that the temperature jump gives rise to the distinctive ramp-like temperature signature that now seems characteristic of temperature (or scalar) fields mixed by sheared turbulence. The existence of this feature was found to be independent of initial conditions. On the basis of the $\theta$ traces, Fiedler (1975) concluded that the turbulent region consists of clearly separated vortex-like lumps. He also used the conditional sampling technique to show that, within those vortical structures, the mean temperature distribution is approximately linear while the fluctuating temperature intensity is nearly homogeneous.

The main aim of the present experimental study is to take advantage of the temperature tagging of the mixing-layer fluid to obtain further information on the large structure. In addition, while it is often asserted in the literature that the large structure in the mixing layer dominates the transport of a scalar and makes large contributions,

at least during the vortex-pairing process, to the turbulent shear stress, there have not been many attempts to quantify these contributions. Hussain & Zaman (1980) found, in a circular jet under controlled excitation, that the large structure made a significant contribution to the average Reynolds shear stress during pairing. Here, cold wires, separated in either the normal or streamwise direction, are used to obtain estimates of the convection velocity of the large structure and its average inclination to the flow direction. Velocity fluctuations $u$, $v$ and the temperature fluctuation $\theta$ were measured with a X-wire/cold-wire arrangement at different positions in the flow. A conditional sampling and averaging technique, based on the occurrence of large-amplitude positive peaks of $\dot{\theta}^3$ ($\dot{\theta} \equiv \partial\theta/\partial t$ is the temporal derivative of $\theta$), is used to detect the large structure. This technique is described in § 3, while the ensemble-averaged signatures of $u$, $v$, $\theta$, $uv$, $u\theta$ and $v\theta$ obtained with this technique are discussed in § 7. The convection velocity of the large structure, as determined by various methods, and the inclination of this structure are presented in § 5 and 6 respectively.

## 2. Experimental set-up

The experimental rig consists of a Hilton air-conditioning unit which includes a variable-speed blower supplying air to a 25·4 × 25·4 cm square duct, two electric coil heaters, a vapour compression cooling unit and a 0·3 m long test section. Downstream of this test section are a diffuser of area ratio 3:1, a settling chamber, a contraction, a second test section of dimensions 25·4 × 25·4 × 1·2 m and a vertical nozzle (contraction ratio 10:1). An aluminium bounding plate 1·25 cm thick, 10 cm wide and 40 cm long with a 2·54 × 25·4 cm slot is fixed at the nozzle exit. The nozzle exit velocity $U_0$ can be varied continuously from 0 to 16·1 m/sec. The traversing mechanism consists of a modified height gauge with a travel of 30 cm and a least count of 0·01 mm mounted on an aluminium frame attached to the side of the tunnel. Figure 1 is a diagram showing the nozzle, mean velocity and temperature profiles measured at different $x/D$, co-ordinates $x$, $y$, and the similarity variable $\eta$ ($\equiv y/x$).

All measurements were made at an exit velocity $U_0$ of 15·1 m s$^{-1}$ (Reynolds number $U_0 D/\nu = 2{\cdot}65 \times 10^4$, where $D$ is the width of the nozzle and $\nu$ is the kinematic viscosity). Measurements of the inclination and convection velocity of the large structure were made when the jet was either heated or cooled. The temperature difference $\Delta\overline{T}_c$ between the potential core fluid and the ambient air was 28 °C and −8·5 °C respectively. Measurements with the X-wire/cold-wire combination were made only for a slightly heated ($\Delta\overline{T}_c = 8{\cdot}15$ °C) jet. Mean- and fluctuating-temperature profiles were measured with a 0·6 $\mu$m Pt–10 % Rh wire (length 0·7 mm) operated with a constant current (50 $\mu$A) anemometer. The sensitivity of the cold wire to the velocity fluctuation was negligible. Fluctuations $u$ and $v$ were measured with an X-wire (6 $\mu$m diameter, length 1 mm) made of Pt–10 % Rh, operated at an overheat ratio of 0·8 using two DISA 55M01 anemometers and 55M10 bridges. The resistance of the two wires was matched to within 0·3 %. The single cold wire was mounted upstream of the X-wire with a longitudinal separation of 2 mm. It was observed that, when the separation was reduced, the wake of the cold wire affected the X-wire readings. Both the cold and X-wires were calibrated in the potential core of the jet using a Comark thermocouple thermometer and a Mensor quartz pressure transducer respectively. Yaw calibration of the X-wire was done by rotation through ± 5° in the potential core to determine the effective

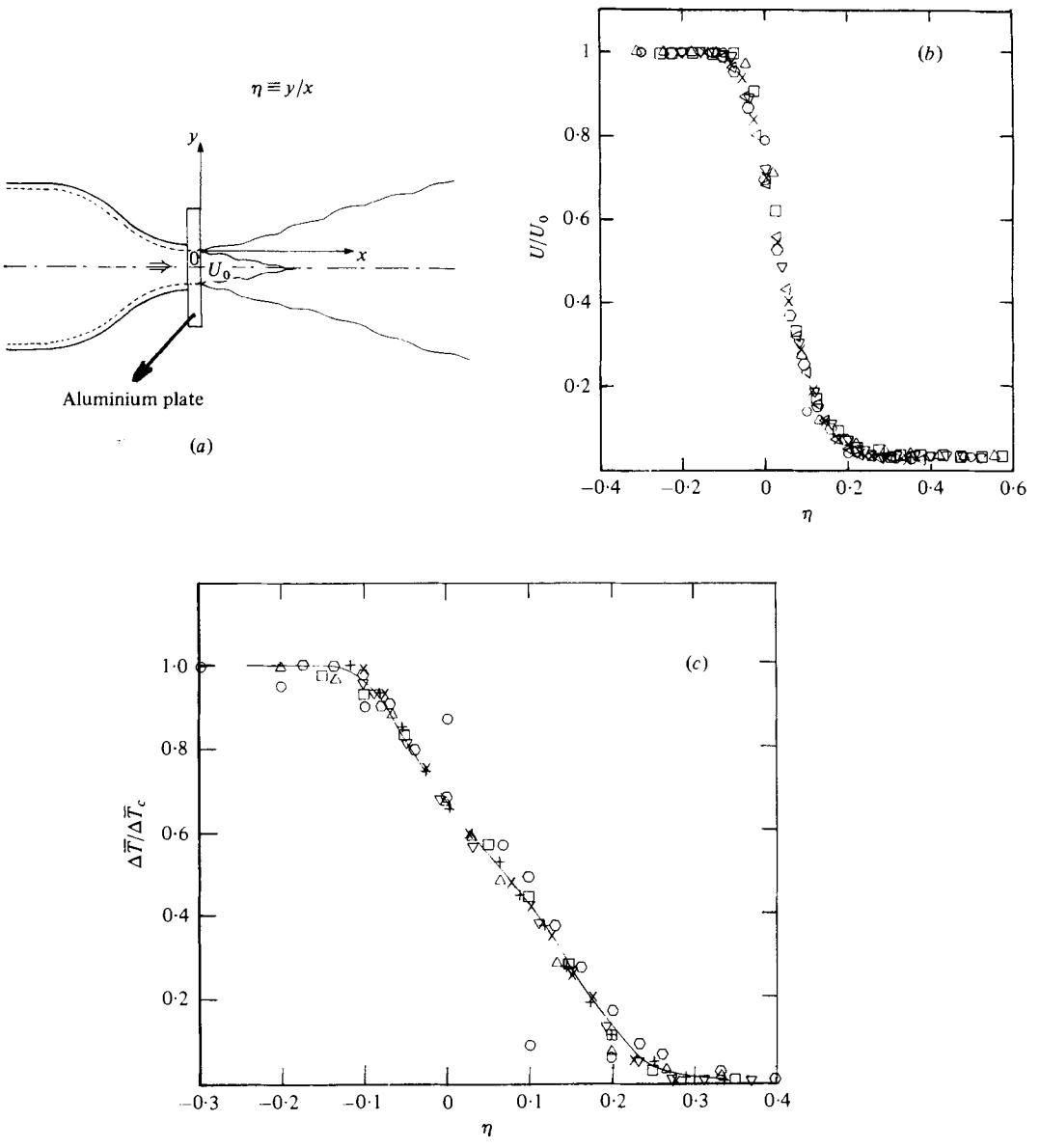


FIGURE 1. (*a*) Sketch of the nozzle and the choice of the co-ordinate system; (*b*) Mean velocity distribution at different $x/D$; ○, $x/D$ = 1·0; △, 1·5; □, 2; ▽, 2·5; ⬡, 3; ×, 3·5; ◁, 4. $U$, local velocity; $\bar{T}_0$, jet exit velocity; (*c*) Mean temperature distribution; $\Delta\bar{T}$, local temperature − ambient temperature, $\Delta\bar{T}_c$, core temperature − ambient temperature.

inclination of the hot wires. The sensitivity of the hot wire to temperature fluctuations expressed as (e.g. Dean & Bradshaw 1976)

$$e_\theta/E = -\tfrac{1}{2}\theta'/(T_w - T_f),$$

where $e_\theta$ is the r.m.s. contribution from the temperature fluctuation to the hot-wire voltage, $E$ is the mean output voltage of the hot-wire bridge, $\theta'$ is the r.m.s. temperature, and $T_w$ and $T_f$ are the average wire and fluid temperatures respectively. As the

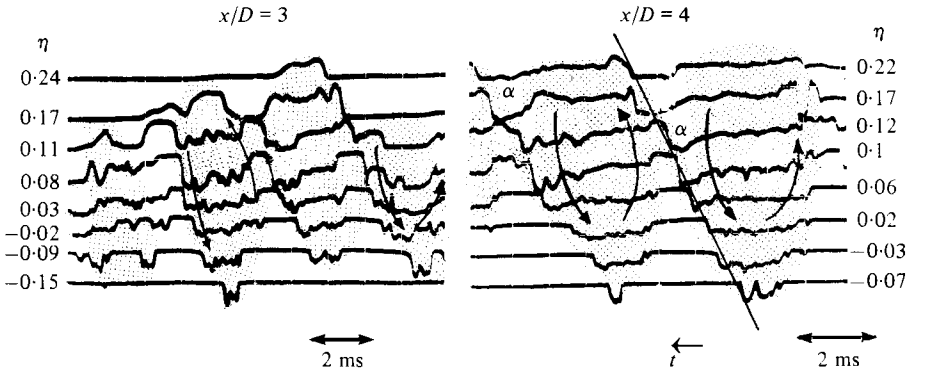


FIGURE 2. Traces of $\theta$ obtained with an eight-wire rake. Shaded regions are tentatively identified with large structures.

maximum error in the uncorrected time-averaged turbulence quantities was less than 2 %, no correction was made to hot-wire readings. Fluctuating voltages from the constant-current bridge and the constant-temperature anemometers were passed through DISA 55D26 signal units, Krohn-Hite filters and analogue buck and gain amplifiers to obtain instantaneous $u$ and $v$ signals; the instantaneous products $uv$, $u\theta$ and $v\theta$ were obtained by using analogue multipliers. The signals were recorded on a Hewlett-Packard 3968 FM tape recorder at a speed of 38·1 cm s$^{-1}$ and later played back at 2·38 cm/sec and digitized using a 10-bit analog-to-digital converter at 8000 Hz (real time).The digital data were processed on a DEC PDP 11/20 computer.

The arrangement used for the convection speed measurements consisted of two cold wires separated by a distance $\Delta x/D = 0{\cdot}3$ with the upstream wire at $x/D = 3{\cdot}0$. Both wires were traversed simultaneously across the heated mixing layer. To obtain the average inclination of the large structure, an array of four cold wires was mounted on the traverse gear. The wires in the array were aligned such that they all were at the same $x$ location. The separation between successive wires was not constant but the wires were positioned to cover the width of the layer, as defined by the velocity range $0{\cdot}1 \leqslant U/U_0 \leqslant 0{\cdot}9$ ($U$ is the mean velocity).

## 3. Detection of the large structure and ensemble-averaging scheme

Figure 2 shows traces of $\theta$ at $x/D = 3$ and 4 obtained with an array of eight cold wires. Lumps of vortical fluid, identified as large structures, are shown as shaded regions. Across the mixing layer, the increase to a higher temperature is noticeably sharper than the decrease to a lower temperature. At the outer edge (low-speed side) the sharp increase is at the front or downstream side of a turbulent bulge, whereas near the core (high-speed side) the sharp increase or rise is associated with the back or upstream side of a bulge. In the central part of the mixing layer, such a clear identification is difficult. A bulge is, for convenience, defined (cf. Sreenivasan, Antonia & Britz 1979) as an excursion in $\theta$ from either ambient or core temperatures. The thin region (or 'braid') connecting two large structures, across which the sharp increase in $\theta$ occurs in the central part of the mixing layer, is treated as an integral part of the large structure. The skewness $S_{\dot{\theta}} (\equiv \overline{\dot{\theta}^3}/\overline{\dot{\theta}'^3}$, where $\dot{\theta} \equiv \partial\theta/\partial t$ and a prime denotes the r.m.s.

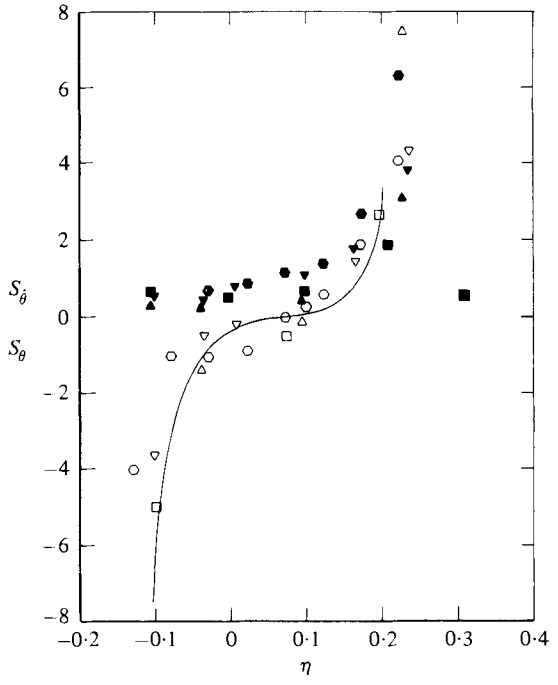


FIGURE 3. Distributions of skewness factors of temperature and its derivative. Open symbols, $S_{\dot\theta}$; filled-in symbols, $S_{\dot\theta}$. △, $x/D$ = 1·5; □, 2; ▽, 3; ○, 4; ——, $S_\theta$, Fiedler (1974).

value) is positive across the mixing layer (figure 3), whereas the temperature skewness $S_\theta$ ($\equiv \overline{\theta^3}/\theta'^3$) is, as expected, negative near the core where $\theta$ exhibits negative excursions and positive on the low-speed side where $\theta$ exhibits positive excursions (figure 2) as a result of heated fluid arriving from the high-speed side of the layer. A positive value of $S_{\dot\theta}$ can be attributed to the sharp increase in $\theta$ which gives rise to a sharp pulse in $\dot\theta$. (When the mixing layer is cooled, the decrease to a lower temperature is sharper than the increase to a higher temperature and hence $S_\theta$ is negative). The sign of $S_{\dot\theta}$ in either the heated or the cooled mixing layer is consistent with the result of Gibson *et al.* (1977)† who observed that the sign of the skewness of the streamwise (spatial) temperature gradient is given by the scalar product of **x** (vector in the streamwise direction) with the cross-product of the mean temperature gradient and mean shear vectors.

On the basis of the appearance of $\dot\theta$ and the positive value of $S_{\dot\theta}$, it seemed appropriate to associate the large-amplitude positive peak of $\dot\theta$ with the signature of the coherent large structure.‡ A similar scheme using $\dot u^3$ was used by Rajagopalan & Antonia (1979) to educe the ensemble-averaged velocity and wall shear stress signatures of the large structure in a two-dimensional duct flow.

Traces of $\dot\theta^3$ and $\theta$ in figure 4 clearly show that large-amplitude peaks of $\dot\theta^3$ are associated with the sharp increase in $\theta$. Although $\dot\theta^3$ has positive and negative peaks,

† It is also consistent with Sreenivasan & Tavoularis' (1980) findings that the sign of the skewness of $\partial\theta/\partial x$ is given by $-\mathrm{sgn}\,(\partial U/\partial y) \times \mathrm{sgn}\,(\partial T/\partial y)$.

‡ Note, however, that the non-zero value of $S_{\dot\theta}$ does not necessarily indicate that small-scale isotropy is violated (e.g. Sreenivasan & Antonia 1977).

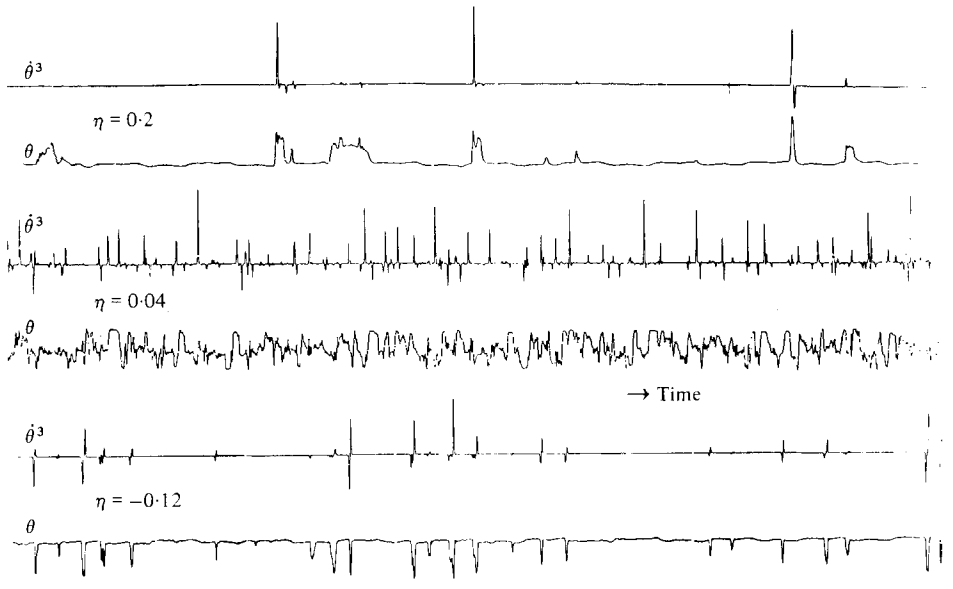


FIGURE 4. Traces of $\theta$ and $\dot{\theta}^3$ at $x/D = 2{\cdot}5$.

positive peaks have, on average, a larger amplitude than negative peaks, consistent with the positive value of $S_\theta$. The ensemble-average shapes of velocity and temperature signatures associated with the large structure were obtained, by computer, after first identifying the locations when the positive peak of $\dot{\theta}^3$ exceeded a predetermined threshold level.† To obtain $\dot{\theta}^3$, $\dot{\theta}$ was first obtained by digital differentiation. Traces of $\dot{\theta}^3$ were computer-plotted and the locations, specified in terms of sampling time intervals, where $\dot{\theta}^3$ reached a maximum immediately after crossing the positive threshold, were identified and subsequently used as inputs to the program that performed the ensemble averaging. The location where $\dot{\theta}^3$ was maximum was arbitrarily taken as $t^* \equiv 0$, and the ensemble averages (denoted by angular brackets throughout this paper) were computed for the first 50 positive and the first 50 negative values of $t^*$ (the time interval between successive points is $\Delta t^* \equiv f_s^{-1}$, where $f_s$ is the sampling frequency). The values of $u$, $v$ and $\theta$ were accumulated at each value of $t^*$ and ensemble averages were later obtained by dividing by the total number of realizations (typically 50). Positive $t^*$ denotes upstream displacement and negative $t^*$ can be identified with downstream displacement. In a few experiments, this number was increased to about 100 but no significant effect on ensemble-average shapes was observed.

## 4. Mean and turbulent flow field

Mean and r.m.s. velocity and temperature profiles normalized by $U_0$ and $\Delta\overline{T}_c$ exhibit reasonable similarity for $2 < x/d < 4$ when plotted as a function of the co-ordinate $\eta$. The growth of the mixing layer is linear with the virtual origin located at the nozzle

† The chosen threshold corresponded to a voltage level equal to $2k$, where $k = (\dot{\theta}^3)'$. Varying the level from $k$ to $5k$ did not have a significant effect on the shape of ensemble averages.

exit plane and with a spread parameter $\sigma$ of 10·2. The untripped boundary layer at the nozzle exit is neither laminar nor fully turbulent, but in a state of transition ($R_{\theta_0} \simeq 145$ where $\theta_0$ is the momentum thickness). The Reynolds number $R_D$ based on centre-line velocity $U_0$ and $x$ varies from $2{\cdot}65 \times 10^4$ to $1{\cdot}06 \times 10^5$ over the range of $x$ considered here. For comparison, values of $R_x$ or $R_D$ for previous experimental investigations are as follows: Dimotakis & Brown (1976),

$$R_x \simeq 3 \times 10^6;$$

Lau & Fisher (1975),

$$2 \times 10^5 < R_x < 6 \times 10^5 \quad (R_d \simeq 2 \times 10^5);$$

Bruun (1977),

$$1 \times 10^4 < R_x < 5{\cdot}3 \times 10^4 \quad (R_d = 2{\cdot}1 \times 10^4),$$

and Yule (1978),

$$9 \times 10^3 < R_d < 2 \times 10^5.$$

($d$ is the nozzle diameter.)

The present X-wire measurements indicate that the distributions of $u'/U_0$ and $v'/U_0$ across the mixing layer are approximately similar for $2 \leqslant x/D \leqslant 4$; the $u'$ distribution is in good agreement with that obtained with a single hot wire. Distributions of $\overline{uv}/U_0^2$, $\overline{u\theta}/U_0 \Delta\overline{T}_c$ and $\overline{v\theta}/U_0 \Delta\overline{T}_c$ are also approximately self-preserving when plotted *versus* $\eta$ for $2 \leqslant x/D \leqslant 4$.

## 5. Convection velocity of large structure

The convection velocity at $x/D = 3$ was obtained from the temperature signals in a number of different ways.

### 5.1. *Average convection velocity*

The space–time correlation of $\theta$, measured with two wires separated by a distance $\Delta x$, is defined as

$$R(\Delta x, \tau) = \overline{\theta_1(t)\,\theta_2(t-\tau)}/\theta_1'\theta_2',$$

where $\tau$ is the time delay and subscripts 1 and 2 denote the upstream and downstream wires respectively. $R(\Delta x, \tau)$ was computed at various positions across the mixing layer. The covection velocity $U_c$ was estimated from the relation $U_c = \Delta x/|\tau_1|$, where $\tau_1$ is the peak time delay, or time delay corresponding to the peak value of $R(\Delta x, \tau)$. $U_c/U_0$ decreases from 0·99 at $\eta = -0{\cdot}13$ to 0·39 at $\eta = 0{\cdot}23$ (figure 5). Very approximately, $U_c$ is smaller or larger than the mean velocity depending on whether $\eta$ is negative or positive. In a circular jet, Brunn (1977), using velocity space–time correlations, obtained $U_c/U_0 = 0{\cdot}67$ at $\eta = -0{\cdot}1$ and 0·62 at $\eta = 0$ for $x/d = 2{\cdot}0$. It should be noted that the convection velocity estimated from $R(\Delta x, \tau)$ is only an average value with equal weighting given to turbulent and non-turbulent regions. Such a convection velocity would also relate to fluctuations averaged over a range of displacements and may differ from that of a material component or interface.

### 5.2. *Convection velocity of fronts and backs*

As the intermittency factor $\gamma$, or fraction of time for which the flow is turbulent, is always less than unity, in the range $1 < x/D < 4$, it is relatively straightforward to determine the convection velocity of the turbulent/non-turbulent interfaces at the edges of a turbulent bulge. The convection velocities $U_F$ (front) and $U_B$ (back) of a

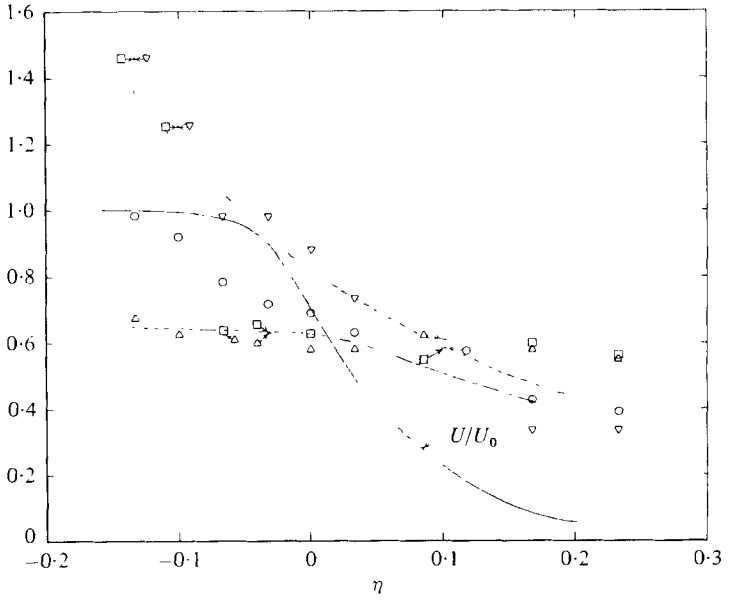


FIGURE 5. Convection velocities at $x/D = 3$, obtained by different methods. ○, $U_c/U_0$, from temperature cross-correlations; □, $U_{c_1}/U_0$, from cross-correlation of $\theta^3$; - - -, $U_F/U_0$; ···, $U_B/U_0$; ▽, $U_D/U_0$; △, $U_R/U_0$; ——, conventional mean velocity, $U/U_0$.

bulge were estimated by first recording, on strip chart, temperature traces from two cold wires separated by a distance $\Delta x$. The time between arrivals of fronts or backs at the wire locations was then estimated by visual inspection of about 100 realizations and the average time delays were determined. The velocity $U_F$ or $U_B$ was then calculated from the ratio $\Delta x/$(average time delay). For $\eta < -0{\cdot}05$, $U_F$ is greater than $U_0$ (figure 5). The ratio $U_F/U_0$ decreases continuously from 1·36 at $\eta = -0{\cdot}14$ to about 0·5 at $\eta = 0{\cdot}17$. The ratio $U_B/U_0$ is approximately constant and equal to about 0·6 for $\eta < 0{\cdot}05$; it decreases to 0·4 at $\eta = 0{\cdot}17$. Accurate determination of $U_F$ or $U_B$ was difficult in the outer part of the mixing layer, as the distinction between turbulent and non-turbulent zones was not sharp. The front of the bulge appears to move faster than the back across the mixing layer but the difference between $U_F$ and $U_B$ is small for $\eta \geqslant 0{\cdot}1$. The difference between $U_F$ and $U_B$ implies that the large-scale structure is continually strained, especially in the region $\eta < 0$. An estimate of the rate of elongation of the structure in this region may be assumed to be proportional to $(U_F - U_B)$. The average convection velocity $\frac{1}{2}(U_F + U_B)$ is approximately equal to $U_c$.

### 5.3. *Convection velocity using* $\theta^3$

The cross-correlation between $\theta^3$ signals at $x/D = 3$ and 3·3 may also be used to estimate the convection speed of the large structure. This method should, like method 5.2, focus on particular features of the large structure, such as the relatively slow decrease and, especially, the sharp rise in temperature. Cross-correlations of $\theta^3$, not shown here, are relatively narrow and sharp as a result of the pulse-like appearance of $\theta^3$ (figure 4). The convection speed $U_{c1}$ was determined, as in method 5.1, once the

peak time delay was estimated. For $\eta < -0{\cdot}1$, $U_{c1}$ (figure 5) is approximately equal to $U_F$ while, for $-0{\cdot}1 < \eta < 0{\cdot}24$, $U_{c1}$ is nearly constant and equal to $0{\cdot}6U_0$.

Another determination of the convection speed of the fronts and backs of the large structure may be obtained by splitting $\theta^3$ into positive and negative parts and computing the cross-correlation between either positive or negative parts. This method should enable the convection speed of the fronts and backs to be determined more accurately than by method 5.2.

For $\eta < 0{\cdot}10$, the convection speed $U_R$ associated with the sharp temperature rise is smaller than the convection velocity $U_D$ associated with the relatively slow decrease. The ratio $U_D/U_0$ decreases from 1·45 at $\eta = -0{\cdot}14$ to 0·34 at $\eta = 0{\cdot}23$. $U_D$ is approximately equal to $U_F$ for $\eta < 0{\cdot}1$ whereas $U_R/U_0$ is constant, equal to 0·6, for

$$-0{\cdot}14 < \eta < 0{\cdot}24.$$

This suggests that the 'cross-over' point where the sharp rise becomes associated with the front of the bulge is at $\eta = 0{\cdot}1$. The traces of figure 2 are consistent with this suggestion. According to Fiedler (1975), entrainment of non-turbulent fluid takes place near those parts of the structure that are identified by a slow decrease in temperature. This corresponds to the front near the core and to the back near the low-speed side. These boundaries move with a velocity larger than the local mean velocity. The boundaries of the structure identified by the sharp temperature rise and associated with little or no entrainment move at a relatively constant velocity. Note that $U_D \simeq U_{c1}$ for $\eta < 0{\cdot}1$ and $U_R \simeq U_{c1}$ for $\eta > 0{\cdot}1$ while, perhaps not surprisingly, the arithmetic mean of $U_R$ and $U_D$ is approximately equal to the mean value of $U_F$ and $U_B$. The reasonably good agreement between convection speeds of fronts and backs, as estimated by methods 5.2 and 5.3, may perhaps be thought to provide some *a posteriori* justification for the technique of first decomposing $\theta^3$ into positive and negative parts and then correlating them to determine $U_R$ and $U_D$.

## 6. Inclination $\beta$ of the large structure

The average inclination of the large structure was obtained by first computing the space–time correlation between temperature fluctuations from any pair of the four-wire rake. Knowing the peak time delay $\tau$ of this correlation, the convection velocity $U_c$, and the distance $\Delta y$ between the wires of the selected pair, the inclination $\beta$ can be determined from $\tan\beta = \Delta y/U_c\tau_1$, where $U_c$ is evaluated at $\Delta y/2$. At $x/D = 2{\cdot}5$, the average value of $\beta$, determined from the space–time correlation between $\theta$ measured by the wire on the low-speed side (largest $\eta$ for the rake) and $\theta$ at one of the other three wires is approximately 35° to the $x$ axis. At $x/D = 3{\cdot}5$, $\beta \simeq 42°$† (figure 6*a*), this increase, relative to $x/D = 2{\cdot}5$, being probably associated with the streamwise growth of the mixing layer. Fiedler (1975) mentioned that the maximum correlation between intermittency functions obtained at locations on opposite sides of the layer where $\gamma = 0{\cdot}5$ was expected to occur at approximately 40° to the $x$ direction.

The inclination of the large structure was also calculated from cross-correlations of $\theta^3$. This estimate of $\beta$ was approximately equal to that obtained from cross-correlations of $\theta$. Low-pass filtering $\theta$ before computing cross-correlations of $\theta$ or $\theta^3$ did not change

† A similar value is obtained when the mixing layer is cooled.

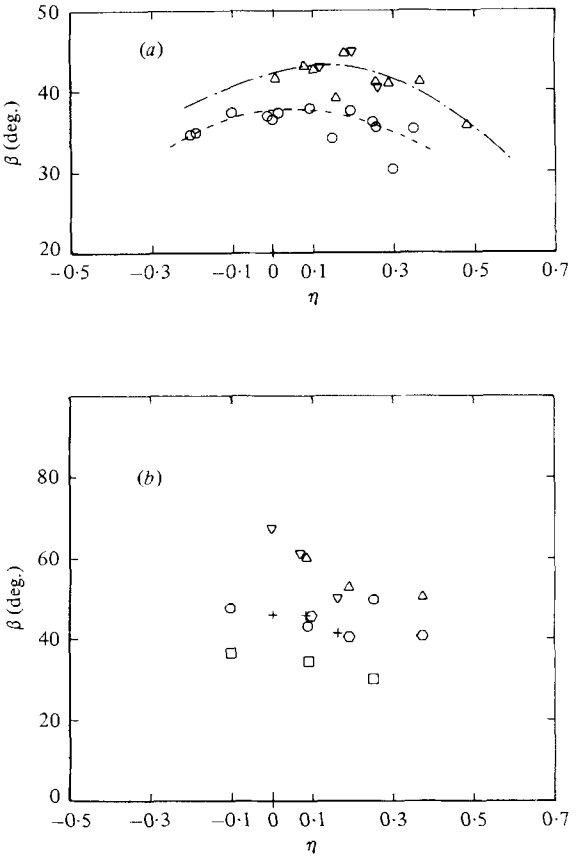


FIGURE 6(*a*). Average inclination $\beta$ of the large structure; ○, $x/D = 2{\cdot}5$; △, 3·5 ▽, 3·5 cooled mixing layer; (*b*). Inclination of parts of the large structure identified by the rise or decrease in temperature. $x/D = 2{\cdot}5$: ○, decrease; □, rise. $x/D = 3{\cdot}5$: ▽, decrease; +, rise. $x/D = 3{\cdot}5$ (cooled mixing layer): ○, decrease; △, rise.

the value of $\beta$ significantly. The inclination $\beta_R$ (or $\beta_D$) associated with the sharp rise (or slow decrease) of the large structure was determined by estimating $\tau_1$ from the cross-correlation of the positive (or negative) parts of $\dot{\theta}^3$ and replacing $U_c$ by $U_R$ (or $U_D$). For the three cases considered (figure 6*b*), $\beta_D > \beta_R$. At $x/D = 3{\cdot}5$, both $\beta_R$ and $\beta_D$ are slightly larger than at $x/D = 2{\cdot}5$. A very rough estimate of $\beta_R$ can be obtained from figure 2 by joining with a straight line the zones of sharp increase in $\theta$ (such a line is shown in the figure) between two successive vortical structures and assuming an average convection speed of $0{\cdot}5U_0$ for these structures. With these assumptions, the line in the figure has an inclination of about 40°. It is reasonably clear from figure 2 that most of the activity is in the thin region connecting consecutive vortex structures. Since it is reasonable to expect this region to dominate $\dot{\theta}$ statistics, it is not surprising that the estimate of $\beta_R$ is in agreement with other estimates of $\beta_R$ given in this section.

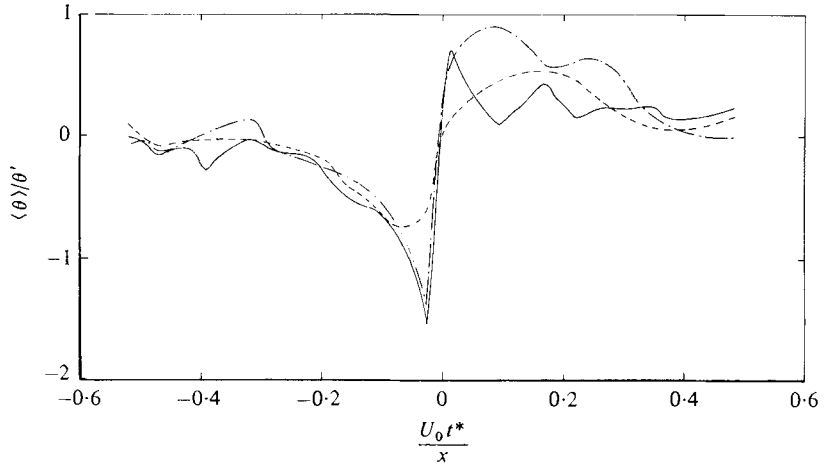


FIGURE 7. Ensemble-averaged shape of $\langle\theta\rangle$ educed from two wires separated in the $x$ direction. Upstream wire is at $x/D = 3$ and $\eta = 0$. ——, $\langle\theta_1\rangle$ educed from upstream wire which is also the detector; - - -, $\langle\theta_2\rangle$ educed from downstream wire when the upstream wire is the detector; · · ·, $\langle\theta_2\rangle$ educed from downstream wire when it is also the detector.

## 7. Ensemble averages

It has already been mentioned in the introduction that, for Lau & Fisher's (1975) experiment, the sampling wire was traversed across the layer downstream of the detecting hot wire. In Bruun's (1977) experiment, the detecting wire was kept within the potential core ($\eta = -0{\cdot}15$) at $x/d = 2$ while the sampling wire was traversed at the same downstream location. The triggering criterion was similar to that of Lau & Fisher and eduction was performed when the positive (or negative) peaks of $u$ exceeded (or fell below) a selected threshold level. Bruun's investigation differed from that of Lau & Fisher in that eduction was carried out for both positive and negative times with respect to the instant when the triggering criterion was satisfied. Yule (1978) used a criterion similar to that of Bruun to educe shapes downstream. The drawback of this type of eduction procedure is that the jitter in the size, shape and convection velocity of the large structure will tend to degrade the educed signature of this structure. Blackwelder (1977) has suggested a correction technique to reduce the effect of jitter on ensemble-averaged shapes. In the present study, no correction technique was applied, but some of the previously mentioned adverse effects were reduced by sampling at the location where the detection criterion is applied.

Figure 7 shows $\langle\theta\rangle$ determined using the horizontally separated temperature wires with the upstream wire located at $x/D = 3{\cdot}0$ and with a separation $\Delta x/D$ equal to 0·3. Whenever positive peaks of $\dot{\theta}_1^3$ (subscript 1 denotes the upstream wire) exceeded $2k$, ensemble averaging was carried out and $\langle\theta_1\rangle$ was determined. A constant time delay, equal to the peak time delay for the $\theta^3$ correlation, was applied to $\theta_2$ before determining $\langle\theta_2\rangle$. At $x/D = 3$ and $\eta = 0$, the initial decrease in $\langle\theta_1\rangle$ is followed by a rapid increase near $t^* = 0$ and a subsequent decrease at large values of $t^*$. Although $\langle\theta_2\rangle$ also exhibits an increase near $t^* = 0$, the rise is not as sharp as that for $\langle\theta_1\rangle$, the difference being probably due to the jitter in convection speed and change of the structure. To reduce

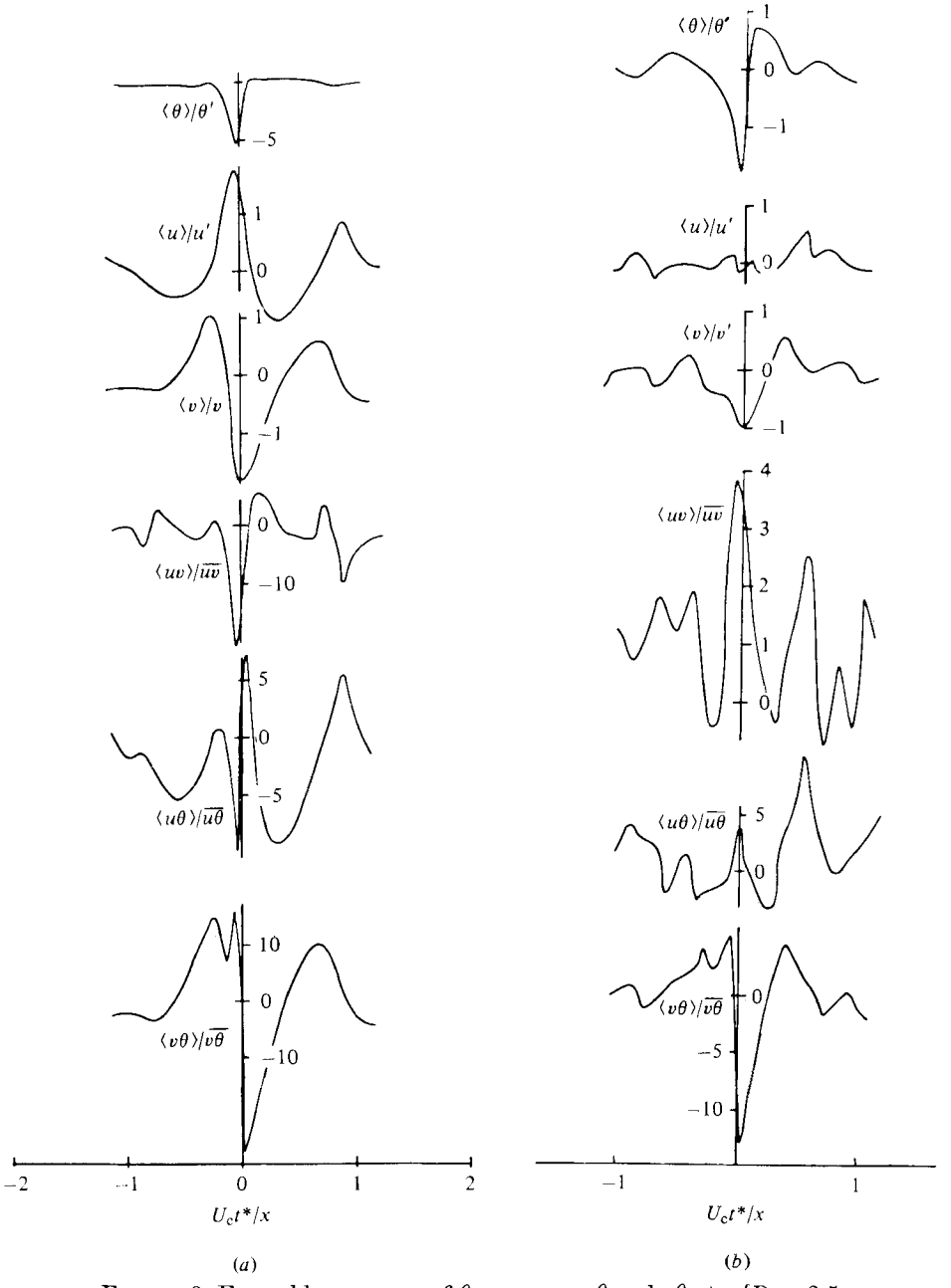


FIGURE 8. Ensemble averages of $\theta$, $u$, $v$, $uv$, $u\theta$ and $v\theta$ at $x/D = 2{\cdot}5$; (a) $\eta = -0{\cdot}12$, (b) $\eta = -0{\cdot}04$, (c) $\eta = 0{\cdot}04$, (d) $\eta = 0{\cdot}2$.

degradation of $\langle\theta_2\rangle$, individual locations of (positive) peaks of $\dot{\theta}_1^3$ and $\dot{\theta}_2^3$ immediately following a crossing of the threshold level ($2k_1$ or $2k_2$) were used to generate the average shapes. The shape of $\langle\theta_2\rangle$ (figure 7), obtained in this fashion, shows a sharp increase at $t^* = 0$. There is, however, a noticeable difference between $\langle\theta_1\rangle$ and $\langle\theta_2\rangle$ for positive values of $t^*$ and this may genuinely reflect changes incurred by the large structure.

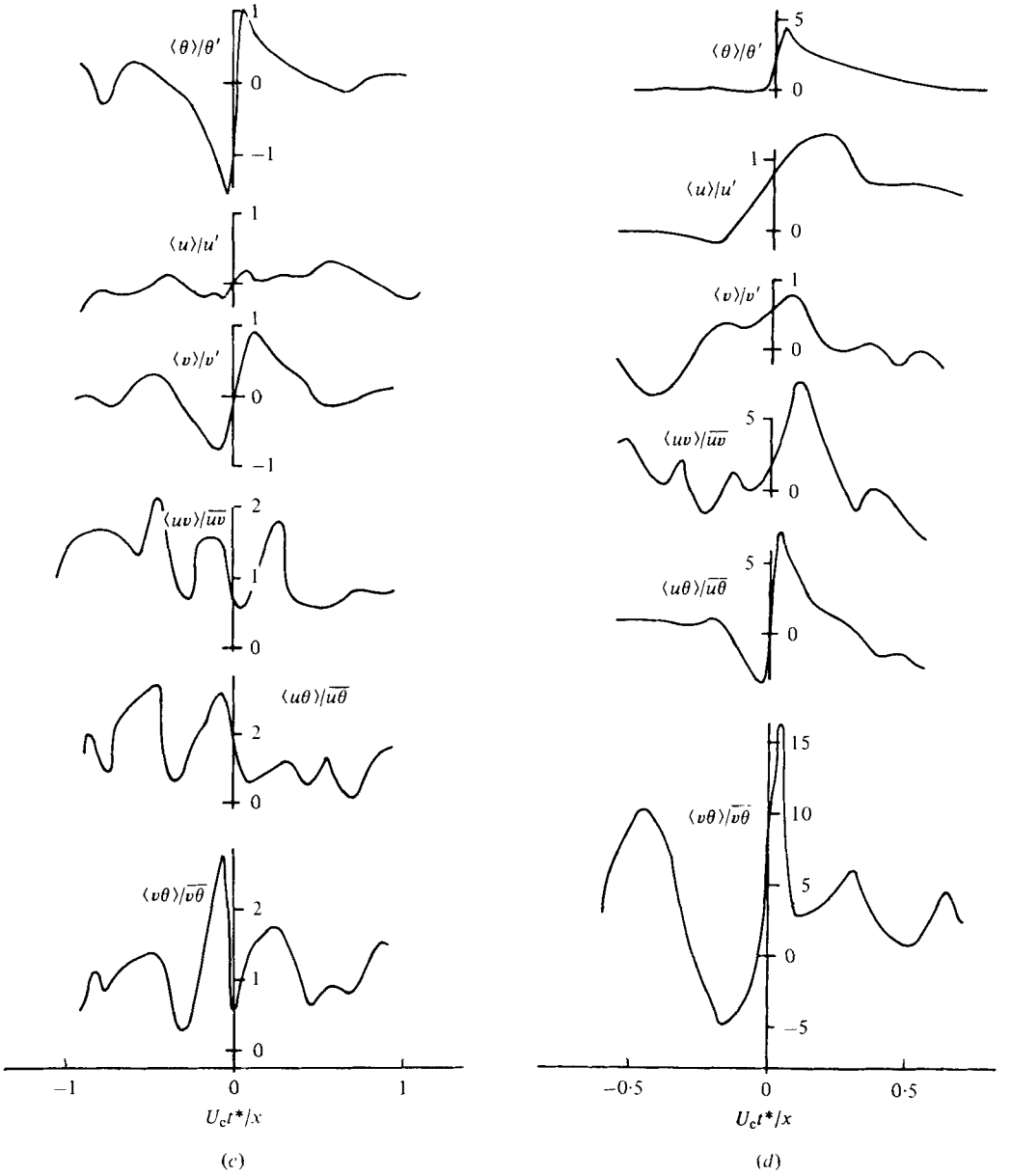


FIGURE 8(*c*, *d*). For legend see p. 274.

Figure 8(*a*)–(*d*) shows shapes of $\langle\theta\rangle$, $\langle u\rangle$, $\langle v\rangle$, $\langle uv\rangle$, $\langle u\theta\rangle$ and $\langle v\theta\rangle$ obtained with the X-wire/cold wire at $x/D = 2{\cdot}5$, for several values of $\eta$. The sharp rise in $\langle\theta\rangle$ is clearly dominant across the mixing layer.† *At* $\eta = -0{\cdot}04$, a large part of the sharp increase lies below the mean level and, at $\eta = 0{\cdot}04$, $\langle\theta\rangle$ is more nearly antisymmetrical about $t^* = 0$.

At $\eta = -0{\cdot}12$, the positive peak $\langle u\rangle$ is larger than the negative peak and occurs near

† When the layer is cooled, the decrease in $\langle\theta\rangle$ is the dominant feature.

$t^* = 0$. The maximum value of $\langle u \rangle$ approaches $2u'$. At $\eta = -0{\cdot}04$ and $0{\cdot}04$, $\langle u \rangle$ does not have a well-defined signature while, at $\eta = 0{\cdot}2$, $\langle u \rangle$ is largely positive and essentially in phase with $\langle \theta \rangle$. It is interesting to note that $\langle v \rangle$ has a relatively well-defined signature at all four values of $\eta$ with a large-amplitude negative peak at $\eta = -0{\cdot}12$ and a relatively sharp increase near $t^* = 0$ at $\eta = -0{\cdot}04$ and $0{\cdot}04$, similar to that observed in $\langle \theta \rangle$. At $\eta = -0{\cdot}12$, the maximum positive value of $\langle u \rangle$ occurs roughly when $\langle v \rangle = 0$. A similar phase relationship between $\langle u \rangle$ and $\langle v \rangle$ was observed by Bruun (1977) in the potential core of a circular jet. However, in the central part of the mixing region and in the low-speed side of the layer, Bruun's results indicate large-amplitude positive and negative peaks respectively for both $u$ and $v$, in contrast with the present observations. It is of interest to compare the present $\langle v \rangle$ distributions at $\eta = -0{\cdot}12$ with the instantaneous $v$ trace (at $\eta = -0{\cdot}11$) presented by Wygnanski & Fiedler (1970). These authors noted that $v$ varied almost linearly with time inside the turbulent flow region and that the values of $v$ at which their probe entered (small $v$) and left (large $v$) the turbulent region seemed to be quite constant. Figure 8(*a*) shows that, for $\eta = -0{\cdot}12$, $\langle v \rangle$ does indeed increase almost linearly for positive $t^*$ but the relatively sharper decrease in $\langle v \rangle$ for $t^* < 0$ seems to be associated with the turbulent region (and not the irrotational flow region), on the basis of the $\langle \theta \rangle$ distribution at this value of $\eta$.

At $\eta = -0{\cdot}12$, $\langle uv \rangle$ has a narrow negative peak at $t^* = 0$ with a maximum value of $-20\overline{uv}$, whereas at other locations $\langle uv \rangle$ has only positive values. At $\eta = -0{\cdot}04$ and $0{\cdot}04$, $\langle uv \rangle$ signatures cannot be described as distinct, when compared with those at $\eta = -0{\cdot}12$ or $0{\cdot}2$. Similarly, $\langle u\theta \rangle$ has a sharp increase at $\eta = -0{\cdot}12$ and $0{\cdot}2$, but does not have a characteristic shape at $\eta = -0{\cdot}04$ and $0{\cdot}04$. This seems consistent with the observation that $\langle u \rangle$ also does not have a distinct signature at $\eta = -0{\cdot}04$ and $0{\cdot}04$. In contrast, $\langle v\theta \rangle$ exhibits a relatively sharp change near $t^* = 0$ at all $\eta$. At both $\eta = -0{\cdot}12$ and $-0{\cdot}04$, the maximum negative value of $\langle v\theta \rangle$ is equal to $25\overline{v\theta}$. Although $\overline{v\theta}$ is positive throughout the mixing layer, $\langle v\theta \rangle$ has a sharp, negative amplitude peak at $\eta = -0{\cdot}12$ and $-0{\cdot}04$, whereas it has positive peaks of approximately $3\overline{v\theta}$ and $16\overline{v\theta}$ at $\eta = 0{\cdot}04$ and $0{\cdot}2$, respectively.

## 8. Contribution of the large structure to fluxes and final discussion

The vortex-like character of the large scale in a mixing layer has been established in the literature, by flow visualization studies and hot-wire measurements. For convenience, the present discussion will be based on a simplified picture (figure 2 may be used as a guide) in which two successive vortical structures are interconnected by a relatively thin turbulent layer. As the result of the vortical motion within one structure, low-speed and low-temperature fluid is transferred to the high-speed and high-temperature side and *vice versa*. This is consistent with the educed shapes of $\langle \theta \rangle$ near the core and near the low-speed side. The interconnecting layer is subjected to rotational strain at the back of the downstream structure and at the front of the upstream structure. It is not always straightforward to identify clearly the interconnecting layer (in figure 2 we have denoted two such layers by $\alpha$). Identification of this layer seems unambiguous when the mixing layer is forced by controlled periodic oscillation.† The

† Hussain & Zaman (1980) found that all the vorticity contours in the near field of an excited circular jet appear as concentrated lumps and no significant vorticity could be measured in the

smoke photographs of Oster *et al.* (1978) show that the width of this layer represents, very roughly, 10 % of the diameter of the large structure. In the context of the present measurements, the interconnecting layer can be identified with the back of the structure near the potential core and the front of the structure near the low-speed side and is interpreted to be an integral part of these structures. Both these boundaries are associated with a sharp rise in $\langle\theta\rangle$, as can be clearly seen in the top traces of figures 8 (*a*) and 8 (*d*). It seems reasonable to associate this layer with a 'shear' layer in view of the concomitant sudden changes in $\langle v\rangle$ and $\langle u\rangle$ (except in the central region). An analogous association was suggested by Chen & Blackwelder (1978) with regard to the back of the large structure in a boundary layer. It is interesting to note that, in this latter flow, the thickness of the 'shear' layer was about $0{\cdot}1\delta$ to $0{\cdot}2\delta$, where $\delta$ is the boundary-layer thickness. In the present flow, the thickness of the interconnecting layer is estimated to be approximately $0{\cdot}1D$. This estimate should be treated with caution, since the separation of 2 mm between the cold wire and the X-wire does not permit fine resolution of the interconnecting region. It should also be noted that the interconnecting layer, although continuously strained, moves at a relatively constant velocity $U_R$.

In the central part of the layer, the sharp increase in $\langle\theta\rangle$ appears to be associated with the back of one structure as well as the front of the next structure. Strictly, the increase in $\langle\theta\rangle$ in the central region of the layer should be associated with the interconnecting turbulent layer and, as such, is not easily identifiable with the boundaries of the large structures. In the following discussion, it should be borne in mind that, as a result of the criterion used in the eduction procedure ($t^* = 0$ corresponds to the sharp increase in $\langle\theta\rangle$), average shapes at $\eta = -0{\cdot}12$, $+0{\cdot}2$ can be associated with only one structure while averages in the central region ($\eta = -0{\cdot}04$ and $0{\cdot}04$) are likely to be related within parts of two consecutive large structures.

Lau & Fisher (1975) attributed the appearance of large-amplitude negative pulses in $u$, near the potential core of a circular jet, to the existence of a cross-flow that brings low-momentum fluid from the low-speed side. At $\eta = -0{\cdot}12$, the present positive peak of $\langle u\rangle$ has a larger amplitude than the negative peak. Bruun (1977) also made a similar observation at $\eta = -0{\cdot}15$, inside the potential core of a circular jet. It appears that the positive peak in $\langle u\rangle$ is due mainly to the flow induced by the vortical structure and is not directly associated with the vortical motion that brings low-speed fluid towards the core. The approximately zero value of $\langle v\rangle$ when $\langle u\rangle$ is maximum at $\eta = -0{\cdot}12$ (figure 8*a*) would seem to support this observation. It should be noted that $\langle u\rangle$, as educed inside the potential core by Lau & Fisher, also has a large-amplitude positive peak. At $\eta = -0{\cdot}12$, $\overline{uv}$ is small but positive, whereas $\langle uv\rangle$ has a long and narrow negative peak. The negative peak is consistent with the shapes of $\langle u\rangle$ and $\langle v\rangle$ at this value of $\eta$. Although the contribution to $\overline{uv}$ by the large structure appears to be

---

'braids' between neighbouring vortical structures. While the 'braid' is stretched between the two vortices, the migration of vortical fluid from the 'braids' to the vortex cores apparently ensures the dilution of the 'braid' vorticity. Oster *et al.* (1978) forced a two-dimensional shear layer by oscillating a thin flat at the end of the splitter plate. The orderly part of the mixing layer was visualized as an array of turbulent vortices interconnected by a thin turbulent layer, inclined to the mean flow direction. This layer was found to be relatively inert with most of the vorticity present in the 'cylindrical' vortices. The interconnecting layer can also be identified in the velocity traces, shown by Wygnanski (1979, his figure 16), obtained from a rake of hot wires.

negative, it is possible that the magnitude of the positive contribution from other turbulence length scales is such as to ensure that the average momentum flux is positive.

$\langle\theta\rangle$, $\langle u\rangle$ and $\langle v\rangle$ are mainly positive at $\eta = 0{\cdot}2$ since the velocity and temperature are larger inside the turbulent region than in the ambient fluid. The ensemble-averaged shape of the products are more distinct in this region. On the low-speed side, the thin zone is identifiable with the front and the sharp increase in $\langle\theta\rangle$. It is evident from figures 8($a$, $d$) that the sharp increase in $\langle\theta\rangle$ is accompanied by relatively slow increases in $\langle u\rangle$ and $\langle v\rangle$. This feature has often been noted in conditional measurements made in the outer part of slightly heated turbulent shear flows.

The constant convection velocity associated with the sharp $\langle\theta\rangle$ front does not seem to support Lau & Fisher's suggestion that the large structure may split and form secondary vortices. Convection velocities greater than $U_0$ on the high-speed side have been observed by Clark & Hussain (1979) and Hussain & Clark (1981). The convection velocity of the fronts is greater than $U_0$ for $-0{\cdot}16 < \eta < -0{\cdot}06$ in the present study. The fact that $U_{c1}$, as estimated from $\dot{\theta}^3$, is equal to $U_D$ (or $U_F$) at $\eta = -0{\cdot}16$ and $-0{\cdot}1$ suggests that the dominant feature of the flow near the potential core is the entrainment of high-speed fluid whereas, for $\eta > -0{\cdot}1$, the near equality between $U_{c1}$ and $U_R$ indicates that the dominant feature of the motion is associated with the sharp temperature increase rather than with the slow temperature decrease.

An approximate measure of the average distance $l$ between the centres of consecutive vortical structures can be obtained by measuring the time between the first zero crossings that occur on either side of the sharp increase in $\langle\theta\rangle$ at $\eta = -0{\cdot}04$ and $0{\cdot}04$. Identifying $l$ with the product of this time and the convection velocity $U_{c1}$ it is found that $l/D \simeq 1{\cdot}5$. Lau & Fisher obtained a value of approximately 1·3 for the ratio $l/d$. Using $l/D = 1{\cdot}5$, the average frequency of occurrence $f_0$ of the large structure is estimated to be approximately 250 Hz. This corresponds to values of $f_0 D/U_0$ and $U_0/f_0 x$ of 0·4 and 1·1, respectively. Temperature spectra at $x/D = 2{\cdot}5$ exhibit a mild peak at this frequency. Spectra obtained in the range $0{\cdot}5 < x/D < 4$ indicate that $f_0$ decreases approximately as $x^{-1}$ so that the ratio $U_0/f_0 x$ is constant and equal to 1·1. The average longitudinal extent $w$ of the large structure at $\eta = -0{\cdot}12$ and $0{\cdot}2$ was estimated from the width of the $\langle\theta\rangle$ signature (top traces in figures 8($a$, $d$)) as inferred from the duration of the excursion of $\langle\theta\rangle$ from the relatively steady base line. At $\eta = -0{\cdot}12$, $w/D \simeq 0{\cdot}6$ and, at $\eta = 0{\cdot}2$, $w/D = 1$, implying an increase in the longitudinal extent of the structure towards the low-speed side. Integral length scales, inferred from temperature spectra, provide further support for this increase.

A rough estimate of contributions to $\overline{uv}$ and $\overline{v\theta}$ by the large structure can be obtained from $\langle uv\rangle$ and $\langle v\theta\rangle$ and a knowledge of the frequency $f_0$ of the structure. Signatures $\langle uv\rangle$ and $\langle v\theta\rangle$ were first integrated over the width of the structure, as determined using $\langle\theta\rangle$. At $\eta = -0{\cdot}04$ and $0{\cdot}04$,† the contributions to $\overline{uv}$ are equal to 0·8 and 0·9 respectively with $U_0/f_0 x \simeq 1{\cdot}1$. Almost the entire contribution to the Reynolds stress is provided by the $\langle uv\rangle$ signature of the large structure. At $\eta = -0{\cdot}12$ and $0{\cdot}2$, the corresponding contributions to $\overline{uv}$ are $-1{\cdot}4$ and $0{\cdot}4$. At $\eta = -0{\cdot}12$, the accuracy in determining $\langle uv\rangle/\overline{uv}$ and $\langle v\theta\rangle/\overline{v\theta}$ is rather poor since $\overline{uv}$ and $\overline{v\theta}$ are very small at this location.

† An accurate estimate of the width of the structure is more difficult at these locations than at $\eta = -0{\cdot}12$ or $0{\cdot}2$.

While the magnitude of the $\langle uv \rangle$ contribution should be treated with caution, the sign of the contribution is reproducible and appears to be genuine. At $\eta = 0{\cdot}2$, values of $\overline{uv}$ and $\overline{v\theta}$ are also small but $f_0$ is more difficult to determine than at the other locations, perhaps as a result of the variation in the vertical extent of the structure (figure 2). The contributions to the heat flux $\overline{v\theta}$ by the large structure at $\eta = -0{\cdot}12$, $-0{\cdot}04$, $0{\cdot}04$ and $0{\cdot}2$ are $-0{\cdot}1$, $0{\cdot}5$, $0{\cdot}9$ and $0{\cdot}3$, respectively. The estimates at $\eta = -0{\cdot}12$ and $0{\cdot}2$ must be considered with caution but estimates in the central part of the layer indicate a significant contribution to the average heat flux by the large structure.

## 9. Summary of results

The main results of the present study obtained in a turbulent mixing layer ($R_D = 2{\cdot}65 \times 10^4$) may be summarized as follows:

(i) The average convection velocity of the large structure is smaller and larger than the local mean velocity for negative and positive values of $\eta$ respectively.

(ii) The convection velocity of the front of the structure, as obtained by various methods, is larger than both the local mean velocity and the convection velocity of the back.

(iii) For $\eta < 0{\cdot}1$, the sharp temperature rise occurs at the back of the large structure while, for $\eta > 0{\cdot}1$, it occurs at the front. The convection velocity of that part of the structure associated with the sharp temperature rise is constant, equal to about $0{\cdot}6U_0$.

(iv) The average inclination to the mean flow direction of the large structure is approximately 40°. The side associated with the relatively slow decrease in $\langle \theta \rangle$ has, on average, a slightly larger inclination than the side associated with the sharp increase in $\langle \theta \rangle$. Some evidence has also been obtained in support of an increase in this inclination with increasing $x$.

(v) The temperature signature of the large structure is more distinct than the velocity ($u$) signature. It is suggested that $\theta$ may be more suitable than $u$ for educing information about the structure since $\langle u \rangle$ does not exhibit a distinct signature in the central part of the layer. Ensemble-averaged shapes of $\langle \theta \rangle$ and $\langle v \rangle$ are reasonably similar throughout the mixing layer and the $\langle v\theta \rangle$ signature is more distinct than that of $\langle uv \rangle$ and especially $\langle u\theta \rangle$. On the low-speed side of the layer, a sharp rise is followed by a relatively slower decrease in temperature whereas, near the high-speed side, a decrease is followed by a sharper increase. In the central part, $\langle \theta \rangle$ is nearly anti-symmetrical with respect to the sharp rise in temperature.

(vi) Ensemble-averaged shapes of temperature and velocity, both longitudinal and normal, appear to be consistent with the vortex-like description of the large structure, as suggested by several investigators.

(vii) In the central part of the large structure, it is estimated that the large structure contributes 80–90 % of the Reynolds shear stress and 50–90 % of the average normal heat flux.

The support of the Australian Research Grants Committee is gratefully acknowledged. The authors would like to thank Prof. A.K.M.F. Hussain and Dr A. J. Chambers for useful discussions of this work.

## REFERENCES


BLACKWELDER, R. 1977 On the role of phase information in conditional sampling. *Phys. Fluids Suppl.* **20**, 232.

BROWAND, F. K. 1975 Ensemble-averaged large scale structure in the turbulent mixing layer. *Turbulent Mixing in Non-Reactive and Reactive Flows* (ed. S. N. B. Murthy), p. 317. Plenum.

BROWAND, F. K. & WEIDMAN, P. D. 1976 Large scales in developing mixing layer. *J. Fluid Mech.* **76**, 217.

BROWN, G. L. & ROSHKO, A. 1974 On density effects and large structure in turbulent mixing layers. *J. Fluid Mech.* **64**, 775.

BRUUN, H. H. 1977 A time-domain analysis of the large-scale flow structure in a circular jet. Part 1. Moderate Reynolds number. *J. Fluid Mech.* **83**, 641.

CHEN, C. P. & BLACKWELDER, R. F. 1978 Large-scale motion in a turbulent boundary layer: a study using temperature contamination. *J. Fluid Mech.* **89**, 1.

CLARK, A. R. & HUSSAIN, A. K. M. F. 1979 On convection velocities in a mixing layer: effects of the initial condition. *Proc. 2nd Symposium on Turbulent Shear Flows*, p. 2.30. Imperial College, London.

DAVIES, P. O. A. L. & YULE, A. J. 1975 Coherent structures in turbulence. *J. Fluid Mech.* **69**, 513.

DEAN, R. B. & BRADSHAW, P. 1976 Measurements of interacting turbulent shear layers in a duct. *J. Fluid Mech.* **78**, 641.

DIMOTAKIS, P. E. & BROWN, G. L. 1976 The mixing layer at high Reynolds number: large structure dynamics and entrainment. *J. Fluid Mech.* **78**, 535.

FIEDLER, H. E. 1974 Transport of heat across a plane turbulent mixing layer. *Adv. Geophys.* A **18**, 93.

FIEDLER, H. E. 1975 On turbulence structure and mixing mechanism in free turbulent shear flows. *Turbulent Mixing in Non-Reactive and Reactive Flows* (ed. S. N. B. Murthy), p. 381. Plenum.

GIBSON, C. H., FRIEHE, C. A. & MCCONNELL, S. O. 1977 Structure of sheared turbulent fields. *Phys. Fluids Suppl.* **20**, 156.

HUSSAIN, A. K. M. F. & CLARK, A. R. 1981 On the coherent structure of the axisymmetric mixing layer: a flow-visualization study. *J. Fluid Mech.* **104**, 263.

HUSSAIN, A. K. M. F. & ZAMAN, K. B. M. Q. 1980 Vortex pairing in a circular jet under controlled excitation. Part 2. Coherent structure dynamics. *J. Fluid Mech.* **101**, 493.

LAU, J. C. & FISHER, M. J. 1975 The vortex-street structure of 'turbulent' jets. Part 1. *J. Fluid Mech.* **67**, 299.

OSTER, D., WYGNANSKI, I., DZIOMBA, B. & FIEDLER, H. 1978 On the effect of initial conditions on the two dimensional turbulent mixing layer. *Structure and Mechanisms of Turbulence I* (ed. H. Fiedler), Lecture Notes in Physics, vol. 75, p. 48. Springer.

RAJAGOPALAN, S. & ANTONIA, R. A. 1979 Interaction between large and small scale motions in a two-dimensional duct flow. *Phys. Fluids* **23**, 1101.

SOKOLOV, M., HUSSAIN, A. K. M. F. & KLEIS, S. J. 1979 A spark-induced turbulent 'spot' in a turbulent mixing layer. *Proc. 2nd Symp. on Turbulent Shear Flows*, p. 11.13. Imperial College, London.

SREENIVASAN, K. R. & ANTONIA, R. A. 1977 Skewness of temperature derivatives in turbulent shear flows. *Phys. Fluids* **20**, 1986.

SREENIVASAN, K. R., ANTONIA, R. A. & BRITZ, D. 1979 Local isotropy and large structures in a heated turbulent jet. *J. Fluid Mech.* **94**, 745.

SREENIVASAN, K. R. & TAVOULARIS, S. 1980 On the skewness of the temperature derivative in turbulent flows. *J. Fluid Mech.* **101**, 783.

SUBRAMANIAN, C. S. & ANTONIA, R. A. 1979 Some properties of the large scale structure in a slightly heated turbulent boundary layer. *Proc. 2nd Symp. on Turbulent Shear Flows*, p. 4.18. Imperial College, London.

SUNYACH, M. 1971 Contribution à l'étude des frontières d'écoulements turbulents libres. Thèse Docteur ès Sciences, Université Claude Bernard, Lyon.

WINANT, C. D. & BROWAND, F. K. 1974 Vortex pairing: the mechanism of turbulent mixing layer growth at high Reynolds number. *J. Fluid Mech.* **63**, 237.

WYGNANSKI, I. 1979 The recognition of an evoked large-scale structure. *Proc. Dynamic Flow Conf. – Dynamic Measurements in Unsteady Flows*, 1978, p. 191. Baltimore, Marseille.

WYGNANSKI, I. & FIEDLER, H. E. 1970 The two-dimensional mixing region. *J. Fluid Mech.* **41**, 327.

YULE, A. J. 1978 Large-scale structure in the mixing layer of a round jet. *J. Fluid Mech.* **89**, 413.